Decomposing CO_2 fluxes measured over a mixed ecosystem at a tall tower and extending to a region: A case study

Weiguo Wang,[1,2] Kenneth J. Davis,[1] Bruce D. Cook,[3] Martha P. Butler,[1] and Daniel M. Ricciuto[1]

Received 20 August 2005; revised 22 January 2006; accepted 30 January 2006; published 17 May 2006.

[1] CO_2 fluxes for six stand types are inferred by decomposing eddy-covariance (EC) fluxes measured at a 447-m tower using footprint models and ecosystem models in a case study. The functional parameters in the ecosystem models are estimated for each stand type utilizing temporal EC flux series. The results show differences in terms of the functional parameters and fluxes among the different stand types that are consistent with general expectations for the respective stand types. The fluxes, in addition to measurements at two nearby short towers, are used for flux aggregation in the region. Comparisons suggest that it is critical for flux aggregation to distinguish the wetland from the upland. A distinction among three upland forests and between forested and lowland wetlands could be important, too. The difference in aggregated values of net ecosystem-atmospheric exchange of CO_2 with the watershed function classification scheme and with the stand-type level classification scheme can reach about 250 gC m^{-2} $season^{-1}$ over the entire growing season. Analyses suggest that the six-stand classification scheme still does not capture all the variability in stand characteristics relevant to CO_2 exchange. In addition, the varying fluxes for the same stand type with location in the region challenge the widely used land-cover-based ecosystem classification scheme. It is improper to use EC measurements at any single tower to approximate CO_2 fluxes in the region. Implications may help identify key ecosystem types and design more measurements in the region. Limitations and future efforts are discussed.

Citation: Wang, W., K. J. Davis, B. D. Cook, M. P. Butler, and D. M. Ricciuto (2006), Decomposing CO_2 fluxes measured over a mixed ecosystem at a tall tower and extending to a region: A case study, *J. Geophys. Res.*, *111*, G02005, doi:10.1029/2005JG000093.

1. Introduction

[2] Terrestrial ecosystems play a critical role in the global carbon cycle. To date, there is still significant uncertainty about how much carbon dioxide (CO_2) is absorbed by terrestrial vegetation and what factors control this process [*Intergovernmental Panel on Climate Change* (*IPCC*), 2001] due to the lack of observations; this leads to large uncertainty in predictions for the future uptake or release of CO_2 in the global environment [*Cao and Woodward*, 1998; *Cramer et al.*, 2001; *Huntingford et al.*, 2000; *IPCC*, 2001; *Pan et al.*, 1998; *Woodward and Kelly*, 1995; *Woodward et al.*, 2002]. Currently, the net ecosystem-atmosphere exchange of CO_2 (NEE) can be inferred on global and somewhat on continental scales by means of inverse modeling [*Bousquet et al.*, 1999; *Ciais et al.*, 1995; *Enting et al.*, 1995; *Gurney et al.*, 2002; *Tans et al.*, 1990], and NEE can also be directly observed on local scales (of order 1 km^2 or smaller) using techniques such as tower-based eddy covariance (EC) [*Baldocchi et al.*, 2001, and references therein]. NEE, however, is rather difficult to measure over regions with mixed land covers between 1 km^2 and the globe in area.

[3] One approach to estimating CO_2 fluxes in a heterogeneous region is to extrapolate flux measurements for each identified ecosystem type to the region with an assumption of similarity of ecosystems based on a classification scheme within the landscape [*Mackay et al.*, 2002]. Given the flux measurements and proportions of the identified ecosystem types that constitute the region, regional fluxes can be estimated. This spatial aggregation is straightforward, but still difficult to carry out in practice owing to the demands of identifying important ecosystem types, and then gathering sufficient information on both the distribution of the ecosystems of all types and the fluxes for each ecosystem type. No general theory exists to determine what level of ecosystem classification is acceptable in terms of both the accuracy of the classification data and the representativeness of the measurements for each ecosystem type. In principle, regional fluxes can be estimated more accurately by conducting measurements for more ecosystem types.

[1]Department of Meteorology, Pennsylvania State University, University Park, Pennsylvania, USA.
[2]Now at Pacific Northwest National Laboratory, Richland, Washington, USA.
[3]Department of Forest Resources, University of Minnesota, Saint Paul, Minnesota, USA.

0148-0227/06/2005JG000093$09.00

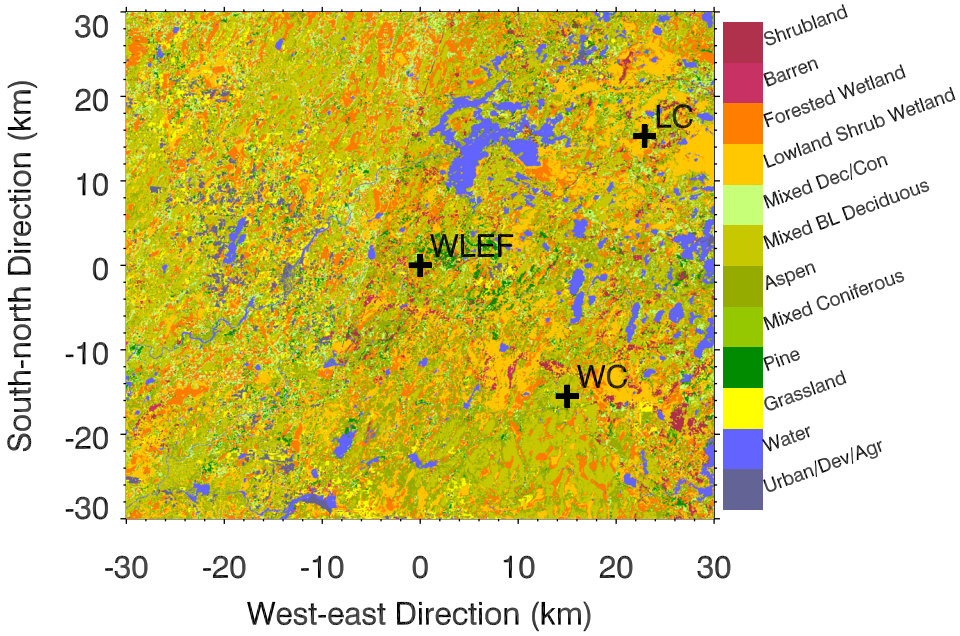

Figure 1. Distribution of land cover classes in the 60 km × 60 km region centered on the WLEF tower (45.9455878°N, 90.272304°W) in northern Wisconsin, USA. The three pluses represent the locations of the WC, LC, and WLEF towers. Data source is WISCLAND [*WiDNR*, 1998]. The flux aggregation is conducted in the 40 km × 40 km area centered at WLEF.

[4] It is, however, usually impractical to make flux measurements for a large number of ecosystem types in a region with mixed ecosystem types. In this regard, tower-or aircraft-based EC flux measurements over a mosaic of mixed ecosystem types can help. Such measurements usually cannot be directly adopted to approximate fluxes in the region because they may not be representative of the fractional coverage of ecosystem types within the region, or may miss some important ecosystem types, but they can be used to infer NEE values for individual ecosystem types since EC fluxes can be interpreted as the weighted averages of the NEE values for all ecosystem types in their footprint areas [*Horst and Weil*, 1994; *Schmid*, 2002] and can be possibly decomposed. It is believed that assigning EC fluxes to multiple individual ecosystem types is a reasonable way to extend tower- or aircraft-based EC measurements to a region and benefits the interpretation of the measurements as well. With the inferred NEE values for more ecosystem types and existing measurements, regional NEE estimates would be more reliable. *Chen et al.* [1999], for example, proposed a scheme to successfully separate aircraft flux measurements into fluxes for specific land cover types. *Ogunjemiyo et al.* [2003] also used a multiple regression model to relate aircraft flux measurements to the fractional distribution of surface land cover types. Both studies indicate that conducting flux decomposition is a promising approach to estimate the NEE values for specific ecosystem types. No similar analyses, however, have yet been applied to tower-based measurements, whose long duration in time can capture long-term flux variability and integrals.

[5] In northern Wisconsin, NEE measurements have been made at three levels on a 447-m-tall tower over a mosaic of upland and wetland ecosystems for several years [*Davis et al.*, 2003]. We attempt to infer the stand-level fluxes for the dominant ecosystems around the tall tower by decomposing the measured EC flux temporal series. One goal of this paper is to demonstrate this decomposition approach. The other is to examine the aggregated fluxes in a region using the decomposed fluxes and existing flux measurements with different classification schemes. A stand-level classification scheme is introduced as the framework for making comparisons and regional flux aggregation. Analyses suggest that there are significant differences among aggregated fluxes based on different classification schemes and measurements at any single EC tower may not approximate CO_2 fluxes in the region.

2. Site and Measurements

2.1. Site Description

[6] The study site is located in the Chequamegon National Forest, centered at a tall communication tower (WLEF-TV) (45.9455878°N, 90.272304°W). The tower is about 15 km east of Park Falls, Wisconsin. A 60 km × 60 km land cover map is presented in Figure 1. The spatial resolution of the map is 30 m. The land cover data provided by WISCLAND (Wisconsin Initiative for Statewide Cooperation on Landscape Analysis and Data) were derived from LANDSAT Thematic Mapper (TM) satellite imagery [*Wisconsin Department of Natural Resources* (*WiDNR*), 1998]. Dominant vegetation types in this region are mixed coniferous and deciduous forests, lowland and wetland forest. Deciduous forests comprise about 70% of the landscape according to the WISCLAND classification scheme [*WiDNR*, 1998]. Topography in the region is flat to gently sloping. More detailed descriptions of vegetation in the

Table 1. Ecosystem Classification

Level 1-Watershed Function Level, Watershed Functions	Level 2-Stand Type Level		
	Ecosystem Types	Land Cover Classes Included	Fractional Area,[a] %
Forested upland	I	coniferous, mixed coniferous and deciduous[b]	14.3
	II	aspen	18.5
	III	other upland deciduous[c]	17.4
Wetland	IV	lowland shrub wetland[d]	18.0
	V	forested wetland[e]	16.2
Others	VI	other land cover classes[f]	15.6

[a]Fractional areas of the six ecosystems in the $40 \times 40 km^2$ region centered at the WLEF tower.
[b]Examples include jack pine, red pine, and white spruce, etc.
[c]Examples include Oak and Maple etc.
[d]This stand type includes woody vegetation, less than 20 feet tall, with a tree cover of less than 10%, and occurring in wetland areas.
[e]This stand type includes wetlands dominated by woody perennial plants, with a canopy cover greater than 10%, and trees reaching a mature height of at least 6 feet [*WiDNR*, 1998].
[f]This stand type includes urban/developed, agriculture, grassland, open water, shrub land, and barren.

vicinity of the WLEF tower can be found in the literature [*Burrows et al.*, 2002; *Davis et al.*, 2003; *Mackay et al.*, 2002].

2.2. Tower-Based Measurements

[7] Fluxes of energy, water, and CO_2 are measured using the EC method at the WLEF, Willow Creek (WC), and Lost Creek (LC) towers (Figure 1). Similar measurement methodology and data processing techniques (including data screening criteria) are applied at the three towers [*Berger et al.*, 2001; *Cook et al.*, 2004; *Davis et al.*, 2003; *Wang et al.*, 2005]. Flux measurements have been conducted at three levels, i.e., 30, 122, and 396 m, on the 447-m WLEF tower since 1995 [*Davis et al.*, 2003]. CO_2 mixing ratio data, traceable to WMO primary standards, are collected at 11, 30, 76, 122, 244, and 396 m [*Bakwin et al.*, 1998]. Air temperature, humidity, wind speed and direction are measured at 30, 122, and 396 m. Other micrometeorological variables, for example, radiation, soil temperature and moisture profiles, are measured at several locations in the region around the tower. Canopy height, while highly variable from stand to stand, reaches a maximum of 20–25 m.

[8] At the WC tower, flux data are collected at 30 m above the ground. CO_2 mixing ratio, wind, temperature and humidity data are collected within and above the canopy which is about 20–25 m tall. Radiation, soil temperature, and soil moisture profiles are measured. The tower is located at a mature upland forested area with mixed deciduous species dominated by sugar maple. Detailed descriptions of the instrumentation and land cover at this site are given by *Cook et al.* [2004]. Similar measurements are conducted at the LC tower that is 10 m tall. The tower is located at a mixed lowland and forested wetland area. Canopy height is typically 1–2 m and consists primarily of alder and willow. Vegetation covers typically within the flux footprints are mixed wetland and upland forests at WLEF, upland deciduous forests at WC, and wetlands at LC.

[9] Flux and micrometeorological data collected in 2000 and 2003 are used in this study. Data in 2001 are excluded because a tent-caterpillar outbreak significantly altered summertime fluxes. Flux data at the WLEF tower in 2002 are not reliable because of an error in the data collection system. In the following analyses, the growing season is defined as the months of May through September.

2.3. Ecosystem Classification

[10] In this study, ecosystems are classified based on plant function and watershed function, following categories that have been shown significant in a study of regional evapotranspiration [*Mackay et al.*, 2002]. Although a detailed classification of land covers is provided in the WISCLAND data product [*WiDNR*, 1998], we regroup them for two major reasons. First, the system of equations to be solved becomes intractable if there are too many unknowns, and the number of unknowns is proportional to the number of land cover types. Therefore any land cover type whose percentage area within the footprints for flux measurements is smaller than 5% is combined with others. Second, likely significant differences in characteristics of NEE within the types of upland forests and within the types of wetlands are taken into account, which potentially alters the results of landscape-scale water and CO_2 fluxes estimated by the aggregation approach. *Mackay et al.* [2002] examined how forest species types in northern Wisconsin affect landscape-scale water fluxes and pointed out that the distinction between aspen and other hardwoods is needed because of high growth rate of the aspen. In consideration of the above factors, the ecosystems are classified into six types (Table 1). The ecosystems are also classified into wetland and upland according to watershed functions as a comparison. In the calculation, CO_2 fluxes for open water and roads are assumed to be zero.

3. Equations and Methods

[11] The vertical turbulent flux for a passive scalar (e.g., CO_2) measured at height z_m can be related to the spatial distribution of surface fluxes through a footprint function [*Horst and Weil*, 1994; *Schmid*, 2002; *Schuepp et al.*, 1990], i.e.,

$$F_m(x,y,z_m) = \int_{-\infty}^{\infty}\int_{-\infty}^{x} F_0(x',y',0) f(x-x',y-y',z_m)dx'dy', \quad (1)$$

where x and y are the horizontal coordinates; F_0 and F_m are the fluxes at the surface and measured at height z_m,

respectively; f is the footprint function describing the contribution of each unit element of the upwind surface area to F_m.

[12] Assuming that the whole ecosystem can be classified into n types and the NEE for a specific ecosystem type is independent of location, we can rewrite equation (1) for the measurement at $(0, 0, z_m)$ when z_m is within the surface layer as

$$F_m(0,0,z_m) \approx \sum_{i=1}^{n} \left[(NEE)_i \times w_i \right], \tag{2}$$

where $(NEE)_i$ is the NEE for the ith type of ecosystem, which is unknown and to be determined; w_i denotes the weight of the NEE for the ecosystem type i to the measured flux, which can be expressed as

$$w_i = \frac{\int_{-\infty}^{\infty}\int_{-\infty}^{0} H(x',y') f(-x',-y',z_m)dx'dy'}{\int_{-\infty}^{\infty}\int_{-\infty}^{0} f(-x',-y',z_m)dx'dy'}, \tag{3}$$

where H is a sign function that is equal to 1 if the ecosystem at location (x', y') belongs to type i, and 0 otherwise. The denominator of equation (3) is approximately equal to 1 when z_m is within the surface layer, and $1 - z_m/h$, where h is the convective boundary layer (CBL) depth, when z_m is above the surface layer in CBL [*Horst and Weil*, 1994]. Given the footprint function and the distribution of ecosystems (and hence w_i), it is theoretically possible to estimate NEE values for the n ecosystem types ($n = 6$ in this study, see Table 1) by solving a set of linear equations as long as the number of the flux measurements for a given time is equal to or greater than the number of the ecosystem types. In practice, flux records from aircraft measurements can be divided into several segments equal to or more than the number of ecosystem types and fluxes for each ecosystem type can be directly solved [*Chen et al.*, 1999; *Ogunjemiyo et al.*, 2003]. For tower-based measurements, implementing such direct decomposition requires fluxes measured simultaneously in the region at several towers or heights, or both, whose total number is at least equal to the number of the ecosystem types. It is, however, impractical to conduct flux measurements at a large number of towers or heights within the study region. Alternatively, we can utilize the long temporal record of continuous tower-based flux measurements. The footprints of the measurements vary with meteorological conditions such as wind direction and stability, leading to time-dependent sampling areas and w_i. Using ecosystem models to express the NEE of CO_2 as functions of environmental variables, we can solve for the parameters in the models for different ecosystems on the basis of equation (2). We call this approach indirect decomposition, for the NEE values are calculated using parameters derived in the ecosystem models. This decomposition can span a long period of time.

3.1. Ecosystem Models

[13] A widely-used rectangular hyperbolic equation [*Ruimy et al.*, 1995] is selected to describe daytime NEE response to light intensity

$$NEE = \frac{\alpha I P_m}{\alpha I + P_m} + R_d, \tag{4}$$

where I is the photosynthetically active radiation (PAR), α is the apparent quantum yield (the slope of the light curve at $I = 0$); P_m is the maximum assimilation rate at saturated PAR, and R_d is the respiration rate that is assumed to be constant in this model.

[14] The ecosystem nighttime respiration rate, R, is usually described as a function of temperature. A review of respiration models is given by *Lloyd and Taylor* [1994]. In this study, the Van't Hoff's exponential model is selected to describe the ecosystem respiration rate at night, which is mathematically equivalent to the widely used Q_{10} equation,

$$R = R_{10} Q_{10}^{\frac{T-10}{T}}, \tag{5}$$

where T is soil or air temperature in degrees C, R_{10} is the reference respiration rate at $T = 10°C$; Q_{10} represents the increase in respiration for every 10 degree rise in temperature. Although more complicated models, for example, considering the effects of moisture, are needed in some cases [*Reichstein et al.*, 2002; *Ricciuto et al.*, 2006], the exponential model is selected for its simplicity to test our decomposition method, as is the light response model equation (4). Simple models, similar to a limited number of ecosystem types, improve the stability of the inversion calculation. The air temperature measured at 30 m on the WLEF tower is used in the calculation in the expectation that it is better representative of temperature in the broad, mixed forest footprint area than the soil temperature measured at any single point.

3.2. Footprint Models

[15] The flux footprint, $f(x, y, z_m)$, can be written as the product of a crosswind-integrated footprint, $f^y(x, z_m)$, and a crosswind concentration distribution function, $D_y(x, y)$,

$$f(x,y,z_m) = f^y(x,z_m) \times D_y(x,y), \tag{6}$$

where x is the upwind distance and y is the crosswind distance from the centerline. Dispersion in the crosswind direction is assumed to be symmetric and D_y is modeled as a Gaussian function of x and the standard deviation of the plume in the crosswind direction (σ_y) [*Horst and Weil*, 1992; *Schmid*, 2002]. $\sigma_y = c_1 x(1 + c_2 x)^{-1/2}$, where c_1 is taken as 0.32 under unstable conditions and 0.16 under near-neutral conditions; c_2 is taken as 0.0004 to consider relatively the large roughness values over the forest [e.g., *Arya*, 1999].

[16] The crosswind integrated footprint function, f^y, is estimated within the surface layer using the model derived by *Horst and Weil* [1994, 1995], which combines solutions from analytical and Lagrangian stochastic dispersion models for the cross-wind integrated concentration distribution for near-surface sources [*Horst*, 1979; *van Ulden*, 1978]. The footprint is a function of the surface roughness length (z_0) and the Monin-Obukhov length (L).

[17] An empirical formula is used to estimate the crosswind-integrated footprint for measurements above the surface layer only under strongly unstable conditions. The formula is derived by adjusting the analytical solution for an idealized CBL to closely match a stochastic model with more realistic atmospheric conditions [*Wang et al.*, 2004].

[18] In this study, the Monin-Obukhov length is calculated using the sensible heat and momentum fluxes directly measured at the tall tower. The roughness length, z_0, and zero-plane displacement, d, are estimated using logarithmic wind profiles for near-neutral conditions. z_0 and d are estimated to be in the range of 0.8 to 1.1 m and 15.5 to 16.4 m, respectively, using the measured wind speeds at 30 and 122 m. Therefore z_0 and d are approximated as 0.9 and 16 m, respectively, for computing the footprints of the measurements in the CBL within which land covers are mostly mixed forested wetlands and uplands. We assume that CO_2 is released or absorbed at the level of d above the surface when footprints are estimated. To a first approximation, z_0 and d are taken as 0.2 and 6 m, respectively, for computing the surface layer footprints in the following calculations as a case study. These values are between those for grasses and forests since footprint areas are covered by both forests and grasses. The reason for picking these values and the sensitivity of results to the surface layer footprint uncertainty will be discussed in section 4.4. CBL height is estimated using the empirical formula derived from radar data during campaigns in 1998 and 1999 at the WLEF tower [*Yi et al.*, 2001].

3.3. Solving the Equations

[19] Substituting equations (4) and (5) into equation (2), we can write the measured daytime fluxes as

$$F_m(t) = \sum_{i=1}^{n} \left[\frac{\alpha_i P_{mi} I(t)}{\alpha_i I(t) + P_{mi}} + R_{di} \right] \times w_i(t), \tag{7}$$

and at night as

$$F_m(t) = \sum_{i=1}^{n} \left[R_{10i} Q_{10i}^{\frac{T(t)-10}{10}} \right] \times w_i(t), \tag{8}$$

where α, R_d, P_m, R_{10}, and Q_{10} with the subscript i represent the parameters defined in the ecosystem flux models for the ith ecosystem type; I, T, w_i and F_m are functions of time t.

[20] The time series of the measured fluxes and estimated weights comprise a set of equations with $3 \times n$ and $2 \times n$ unknowns for daytime and nighttime cases, respectively. As long as the number of the equations is greater than or equal to the number of unknowns, the unknowns can be determined. In this study, we used the Levenberg-Marquardt algorithm [*Rodgers*, 2000], which combines the steepest descent and inverse-Hessian function fitting methods, to find the optimal solutions for the nonlinear equations by minimizing the following objective function:

$$J = \sum_{j=1}^{N} \frac{\left(y_j - Y_j\left(\vec{p}\right) \right)^2}{\sigma_j^2} + \beta \sum_{k=1}^{Np} \frac{(p_k - P_k)^2}{{\sigma'_k}^2}, \tag{9}$$

where N is the total number of the data points; N_p is the number of the parameters ($\vec{p}$: p_1, p_2, ..., p_{Np}) (unknowns) of the model; y_j is the measured flux; Y_j is the modeled flux with the N_p parameters; P_k is the prior information for the k-th parameter, which is estimated by fitting equations (4) and (5) to the same data during a period of time and served as the first guess value; σ_j and σ'_k are the standard deviations of y_j and P_k, respectively. The second term on the right-hand side of the above equation can be interpreted as the extended data used to constrain the solution [*Enting*, 2002]. Since we are uncertain about how to quantify errors in the measured fluxes and the simulated footprints, all standard deviations are assumed to be equal in the following experiments. The nonnegative parameter β is introduced to adjust the weight of the prior information. The solutions are in general closer to the prior values as the value of β increases. Not many stable solutions can be obtained if β is too small for the cases at night. Numerical experiments suggest that the solutions can distinguish the parameters among the ecosystem types with β of 0.1 (day) and 1 (night) (note that the first guess values of each parameter are the same among the different ecosystem types). The central values and uncertainties for the solved parameters are estimated as the arithmetic mean and the standard deviation of the results for an analyzed period such as a month. This calculation is performed on blocks of data that are seven days to a few weeks long, depending on the availability of the data.

3.4. Optimal Selection of Data

[21] Owing to the limited amount of the valid flux data and the availability of reliable footprint estimates, flux measurements at three levels are combined to use. Gaps with no valid flux data exist especially at the upper levels because of the logistics of servicing instruments on the WLEF tower and harsh environmental conditions [*Davis et al.*, 2003]. During the growing seasons of the two study years, roughly 80%, 38%, and 35% of hours had available CO_2 fluxes from 30 m, 122 m, and 396 m of the tower, respectively, when the Monin-Obukhov length can be estimated. With the availability of CBL depth being considered, only 8% and 9% of the time had available CO_2 fluxes for 122 m and 396 m levels, respectively. Unfortunately, not all of those available three-level flux measurements can be used to estimate the weights (equation (3)) in that footprint estimates either cannot be made currently or are questionable in some cases. Therefore data are selected and the selection criteria are different in the day and at night, depending on footprint estimates and data availability.

3.4.1. Daytime

[22] Typical fetches of flux footprints are approximately 10 times measurement height above the source level under strong convective conditions, and 100 times in neutral conditions [*Horst and Weil*, 1992; *Schmid*, 2002]. Fetches of footprint for flux measurements at 122 and 396 m, which can be a few kilometers, are larger than those at 30 m (hundreds of meters to 1 km) (see an example of comparison of footprints and source areas at the three levels under unstable conditions [*Wang et al.*, 2004]). Unfortunately, quantifying the footprints above the surface layer has not been studied extensively and models for practical uses are not well developed. In this study, footprints are estimated only under strongly unstable conditions ($|L/h| < 0.1$). As a result, the available flux data under other stability conditions cannot be used. In this case, only 10% of the daytime hours both had available flux measurements and had estimated CBL depth for each of the two high levels. The 30-m-level measured fluxes roughly 80% of the daytime. However, under strongly convective conditions it is likely

that the 30-m level could be influenced significantly by the clearing (grassy area) around the tower with a radius of roughly 150 m; this is special for this tall tower site. In this case, the weights for some of the ecosystem types under study can be too small, which bring difficulties in solving the equations. In addition, it is uncertain to use the surface layer model to estimate footprint for the 30-m level because the footprint area is covered by mixed grasses and forests under strongly unstable conditions and the requirement for application of the footprint model (homogeneous flows) may be seriously violated. Therefore the available 30-m flux data are used only under weak unstable to neutral conditions ($-L >$ 100 m) (about 50% of the daytime hours) in the day, while 122 m and 396 m (often above the surface layer) data are used only under strongly unstable conditions. This selection is similar to the discussion by *Davis et al.* [2003] about optimal algorithm for computing WLEF NEE.

3.4.2. Nighttime

[23] At night, only data measured at 30m are used because the 122-m and 396-m levels are near or above the top of the nocturnal boundary [*Yi et al.*, 2001] and most likely decoupled from the surface [*Davis et al.*, 2003, Figure 1]. Another reason is that the footprints for the two high levels cannot be quantified. The selected data are limited to near-neutral conditions ($L >$ 300 m) because current footprint models are not well defined and the flux measurement is often decoupled from the surface under very stable conditions. Roughly 27% of nighttime data are retained. Typical fetches of nighttime flux footprints are 100 times or greater than measurement height above the source level.

4. Results

[24] Results based on WLEF and WC data for 2000 and 2003, and LC data for 2003 (the tower was installed in the midst of the 2000 growing season) are combined to conduct statistical tests. Unpaired and paired *t*-test methods are used for comparing the results between sites, and among the ecosystems in the WLEF footprint area, respectively. Parameters are considered significantly different when *p*-values are smaller than 0.05, and slightly different when *p*-values are between 0.05 and 0.32, where *p* is the probability that the null hypothesis was true [*Ott*, 1993].

4.1. Daytime Parameters for Different Ecosystems

[25] The parameters are estimated using the hourly-mean data grouped in windows of seven consecutive days. The window is sequentially marched through the data record by increments of 1 day for the time period from May through September in each of the 2 years. For any period of data, all available daytime data (PAR > 0) based on the criteria in section 3.4 are selected. Solutions are rejected (about 30%) if they exceed the range of reasonable values from the literature: $-1 < \alpha < 0$, $0 > P_m > -100$ μmol $m^{-2}s^{-1}$, and $0 < R < 15$ μmol $m^{-2}s^{-1}$ [*Ruimy et al.*, 1995].

4.1.1. Seasonal Patterns

[26] As an example, seasonal patterns of all ecosystem model parameters derived from data collected during the growing season of 2000 are shown in Figure 2. Light-saturated assimilation and daytime respiration rate peak generally in summer for all ecosystems. The patterns are similar to those derived from the WC flux measurements. In contrast to those parameters, not all the apparent quantum yields, α, of the ecosystems vary significantly with season, which is consistent with what is reported in many other studies [e.g., *Luo et al.*, 2000; *Nilsen and Sharifi*, 1994].

4.1.2. Seasonal Average Apparent Quantum Yield, α

[27] No significant differences in the seasonal average quantum yields estimated for the ecosystems (types I–VI) in the WLEF footprint area and observed at the tower sites are found (Table 2). The overall value of the average quantum yield is about −0.05 μmolC/μmol quanta.

4.1.3. Seasonal Average Light-Saturated Assimilation Rate, P_m

[28] In the WLEF footprint area, the forested wetland ecosystem (type V) and aspen ecosystem have larger magnitudes of light-saturated assimilation rates (P_m) than the others (Table 2). The aspen ecosystem has the largest P_m among the three upland forest ecosystems (types I, II, and III) in the WLEF area, implying (1) strongest potential for CO_2 uptake in the day and (2) different responses of the various upland ecosystems to the same environmental conditions. The second implication is significant for aggregating fluxes from stand levels to regions.

[29] The magnitude of P_m of the aspen ecosystem (type II) is significantly larger than that of the mature upland deciduous forests (type III), consistent with the high growth rate of aspen relative to later successional species such as maple and supporting the need to distinguish between aspen and later successional deciduous forests for flux aggregation in this region as reported in a previous evapotranspiration study [*Mackay et al.*, 2002]. The light-saturated assimilation rate measured at the WC upland deciduous site is close to that inferred for the aspen ecosystem in the WLEF area, but larger than that for the mature upland deciduous forests (type III).

[30] With respect to the wetland ecosystems, the forested wetland ecosystem has a larger magnitude of P_m value than the lowland shrub wetland ecosystem. The light-saturated assimilation rate measured at the LC site (most similar to the lowland shrub wetland ecosystem) is smaller than that of the same ecosystem type in the WLEF area. The "other" category, a mixture of shrub, grassland, agriculture, etc., has a small value of $|P_m|$ compared to forested ecosystems.

4.1.4. Seasonal Average Daytime Ecosystem Respiration Rate, R_d

[31] The intercept of the light response curve when PAR is equal to zero, i.e., R_d in equation (4), can be interpreted as the mean respiration rate of an ecosystem in the day, which is one of methods used to estimate the respiration rate despite uncertainty [*Ruimy et al.*, 1995]. The respiration rates estimated for all three types of upland forest ecosystem (types I, II, and III) in the WLEF footprint area are larger than the rate derived using data measured at the WC upland deciduous forest site. Similarly, the respiration rates for both types of wetland ecosystem (types IV and V) in the WLEF footprint area are significantly larger than that for the wetland ecosystem at the LC site, respectively. Those comparisons imply that the respiration rates measured at WC and LC differ in some ways from the corresponding types of ecosystem in the WLEF footprint area. This presents serious difficulty for regional upscaling according to the land-cover-based ecosystem classifications.

[32] Among the six types of ecosystem in the WLEF footprint area, not all the inverted results show statistically

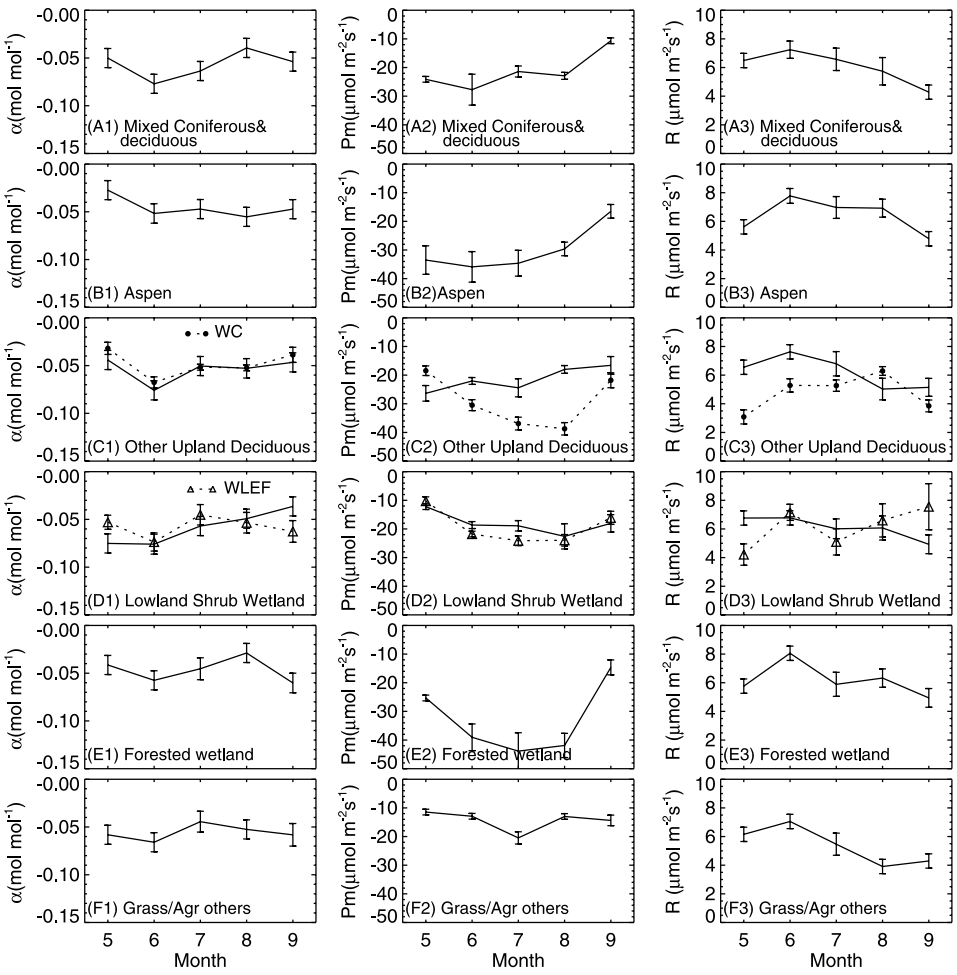

Figure 2. Monthly variation of the inferred functional parameters in the light-response model (equation (4)) for the six ecosystem types in the WLEF footprint area in the growing season in 2000. The parameters fitted to the WC and undecomposed WLEF tower data (dotted lines) are also shown for comparison. The error bars are the standard deviations of the means.

significant differences in R_d. Because of the critical role of respiration in the regional carbon cycle, the respiration rates are further analyzed using nighttime data in the next section, which may be more robust.

4.2. Nighttime Functional Parameters for Different Ecosystems

[33] Nighttime data (PAR = 0) based on the criteria in section 3.4 are selected to estimate the parameters in the respiration model for the six ecosystem types. The selection criteria result in many nighttime data points being screened out. As a result, the data window width is expanded to 20 days to ensure that sufficient data points are available to solve the set of equations. April through October data are utilized in these analyses. The results are rejected (about 40%) if they do not meet the following criteria: $0 < R_{10} < 15$ μmol $m^{-2}s^{-1}$ and $0 < Q_{10} < 4$ [*Ruimy et al.*, 1995].

Table 2. June to August 2000 and 2003 Averages and Standard Errors of the Three Parameters, α, P_m, and R_d, in the Light-Response Model (Equation (4)) for the Six Ecosystem Types in the WLEF Footprint Area[a]

Stand Type or Tower Name[b]	α, μmolC/μmol quanta	P_m, μmolC/m^2/s	R_d, μmolC/m^2/s
I. mixed coniferous/deciduous	−0.051 ± 0.004	−28.6 ± 1.8	6.4 ± 0.3
II. aspen	−0.046 ± 0.004	−38.9 ± 2.4	7.1 ± 0.3
III. other deciduous	−0.054 ± 0.004	−24.5 ± 1.4	6.8 ± 0.4
IV. lowland wetland	−0.052 ± 0.004	−23.5 ± 1.9	6.4 ± 0.3
V. forested wetland	−0.048 ± 0.003	−34.8 ± 2.3	6.2 ± 0.3
VI. others	−0.056 ± 0.003	−13.5 ± 0.6	5.0 ± 0.2
Willow Creek tower	*−0.055 ± 0.002*	*−37.3 ± 1.1*	*4.9 ± 0.2*
Lost Creek tower	*−0.055 ± 0.003*	*−12.5 ± 0.2*	*3.5 ± 0.1*

[a]In this case, results in May and September are not included to reduce the seasonal variability in the comparisons of the parameters among ecosystem types. The parameters fitted to the WC and LC data are also shown. CO_2 fluxes for open water and roads are assumed to be zero.

[b]Tower names are italicized.

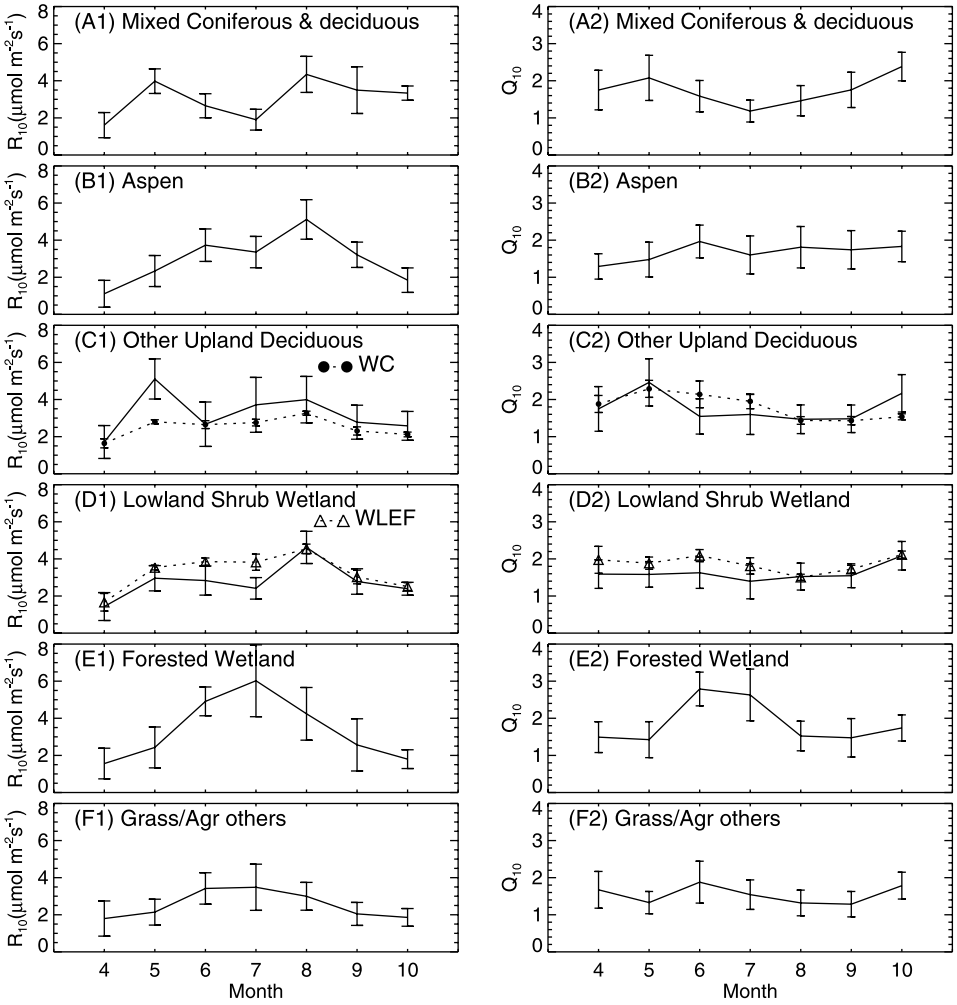

Figure 3. Monthly variation of the inferred functional parameters in the respiration model (equation (5)) for each ecosystem type in the WLEF footprint area from April to October in 2000. The parameters fitted to WC and undecomposed WLEF data are also shown for comparison. This analysis uses only nighttime flux data. The error bars are the standard deviations of the means.

4.2.1. Seasonal Patterns

[34] As expected, R_{10} is generally larger in the growing season than in the dormant season (Figure 3). The average values of R_{10} for the six ecosystem types in the WLEF area vary from 2 to 6 μmol $m^{-2}s^{-1}$ in summer. In general, both observed and inferred Q_{10} values are not a strong function of the season, indicating little change in the sensitivity of respiration to temperature across seasons. This result suggests that the respiration could be sensitive to other factors such as soil moisture and wetland water table depths at this mixed wetland and upland site. Preliminary research implies that soil moisture may be a significant factor in describing ecosystem respiration in the region [*Ricciuto et al.*, 2006].

4.2.2. Seasonal Average R_{10}

[35] The growing season average R_{10} observed at the WC site is smaller than those of the footprint-decomposed mixed coniferous and deciduous forests (type I) and aspen forests (type II) in the WLEF footprint area, and slightly smaller than that for the mature deciduous forest ecosystems (type III) (Table 3). With respect to wetland ecosystems, R_{10} at the LC site is smaller than those for both wetland ecosystems (types IV and V) in the WLEF footprint area.

4.2.3. Seasonal Average Q_{10}

[36] There is no significant difference between the Q_{10} values for the WC and LC sites. Among the upland forest ecosystems (types I, II, and III) in the WLEF footprint area, the aspen ecosystem has the largest Q_{10}. The lowland wetland (type IV) has a smaller Q_{10} value than the forested wetland (type V). The forested wetlands have a Q_{10} similar to the upland forest ecosystems. These comparisons imply that the sensitivities of respiration to temperature change may be different among the upland forests with different functional types and species, and between the different wetland types.

[37] In addition, the WC site has a Q_{10} similar to the upland forest ecosystems (types I, II, and III) and the forested wetland ecosystem in the WLEF footprint area. The LC site has a larger Q_{10} than the lowland shrub wetlands (type IV), but the value is similar to the forested wetlands (type V), in the WLEF footprint area, implying that the responses of similar stand types may vary at different sites.

Table 3. Averages and Standard Errors of the Two Functional Parameters, R_{10} and Q_{10}, in the Respiration Model (Equation (5)) for Each Ecosystem Type in the Growing Seasons (May Through September) in 2000 and 2003[a]

Ecosystem Type or Tower Site Name[b]	R_{10}, μmolC/m^2/s	Q_{10}
I. mixed coniferous/deciduous	3.2 ± 0.25	1.7 ± 0.10
II. aspen	3.7 ± 0.25	1.9 ± 0.10
III. other deciduous	3.1 ± 0.34	1.7 ± 0.09
IV. lowland wetland	2.9 ± 0.20	1.6 ± 0.05
V. forested wetland	3.6 ± 0.40	1.9 ± 0.11
VI. others	2.7 ± 0.23	1.5 ± 0.07
Willow Creek tower	*2.7 ± 0.06*	*1.8 ± 0.08*
Lost Creek tower	*2.0 ± 0.15*	*1.9 ± 0.14*

[a]Parameters fitted to the two stand-level towers (WC and LC) are also shown. Only nighttime flux data are used in this analysis. CO_2 fluxes for open water and roads are assumed to be zero.
[b]Tower names are italicized.

4.3. Comparison of Daily Integrated Fluxes

[38] Figure 4 shows the May through September average, integrated daily NEE, ecosystem respiration (ER), and gross ecosystem production (GEP) estimated for the six ecosystem types in the WLEF footprint, as well as these same products for the WC, LC and un-decomposed WLEF tower data. The respiration model (equation (5)) and parameters derived using nighttime data are used to calculate daytime ecosystem respiration. NEE values are calculated by using equations (4) and (5) during the daytime and at night, respectively. In the calculation, the missing parameters of days are approximated as the respective monthly mean values. The gross ecosystem production is calculated by subtracting the daytime respiration rate from the daytime NEE of CO_2, i.e., GEP = NEE − ER. The error bars represent the estimated standard error due to the variation of the daily integrated fluxes (resulted from variation of environmental variables and derived model parameters).

4.3.1. Average Daily Ecosystem Respiration, ER

[39] Among the three tower sites, the highest and lowest ER values are observed at the WLEF and LC sites, respectively (Figure 4a). ER for the upland deciduous forest at the WC site is smaller than ER for the three upland forest stand types (types I, II, and III) in the WLEF footprint area. Aspen shows the highest ER among upland forest types. Forested wetlands (type V) exhibit the highest ER among wetland types. The lowland shrub wetland ecosystem (type IV) has a larger ER than the LC site. The comparison indicates that ER differs among upland forest ecosystem types and between wetland ecosystem types, as well as between similar ecosystem types at different sites.

4.3.2. Average Daily Gross Ecosystem Production, GEP

[40] The highest GEP (in magnitude) is observed at the WC site, with the lowest value being at the LC site. The WLEF site has an intermediate average daily GEP (Figure 4b) in contrast to its high ER among three tower sites. Aspen (type II) and forested wetland (type IV) exhibit a GEP similar to the WC site. The mixed coniferous and deciduous (type I) and other upland deciduous forest (type III) types have somewhat lower GEP.

[41] The magnitude of the average daily GEP for the lowland shrub wetland ecosystem measured at the LC tower is slightly smaller than that for the same ecosystem type inverted in the WLEF footprint area (type IV), both of which have smaller GEP than the forested wetland ecosystem (type V).

4.3.3. Average Daily Net Ecosystem-Atmosphere Exchange, NEE

[42] Among the three tower sites, the WC site has the highest net uptake of CO_2 followed by the LC site. The net uptake of CO_2 (|NEE|) measured at WLEF site is the smallest. Among the six ecosystem types in the WLEF footprint area, the mixed coniferous and deciduous ecosystem (type I) has a slightly larger |NEE| than the other two upland forest ecosystems. |NEE| for the forested wetland ecosystem (type V) is larger than that for the lowland shrub wetland ecosystem (type IV) and nearly equal to that for the mixed coniferous and deciduous upland forest ecosystem (types I) in the WLEF footprint area. All forested upland ecosystems and the lowland shrub wetland ecosystem (type IV) have smaller |NEE| values in the WLEF footprint area than the ecosystems at the WC site and at the LC site, respectively.

4.4. Impacts of Surface Layer Footprint Uncertainty on Solutions

[43] To test how sensitive the derived ecosystem model parameters are to the surface layer footprint, we compared the results using different simulated footprints through changing footprint model parameters (z_0, d, and σ_y). We calculate the footprints for measurements in the surface layer with the following values of z_0 and d in an increasing order of the footprint area at a given stability: (1) z_0 = 0.5 m and d = 15 m; (2) z_0 = 0.4 m and d = 10 m; (3) z_0 = 0.3 m and d = 8 m; (4) z_0 = 0.2 m and d = 6 m; (5) z_0 = 0.1 m and d = 4 m. Meanwhile, footprints are also computed with two

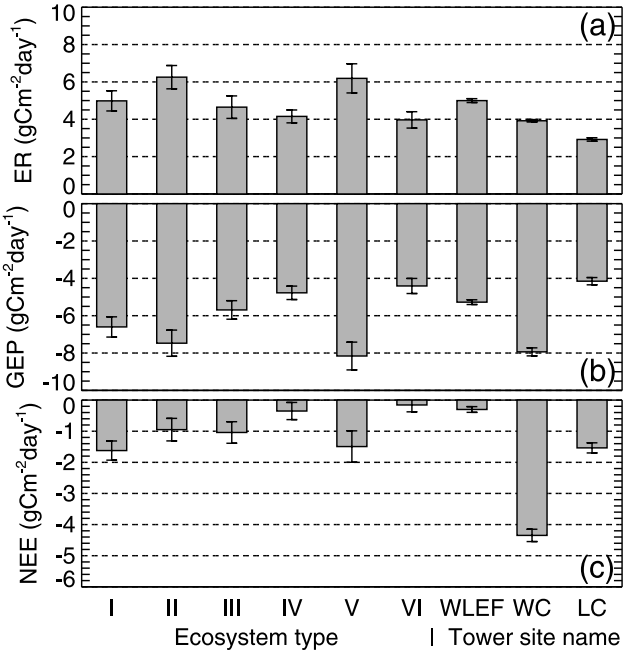

Figure 4. Average daily integrated (a) ecosystem respiration flux, (b) gross ecosystem production, and (c) NEE, over the period of the growing seasons (May through September) in 2000 and 2003. Note that the Lost Creek data are not available in 2000. The error bars are the standard deviations of the means.

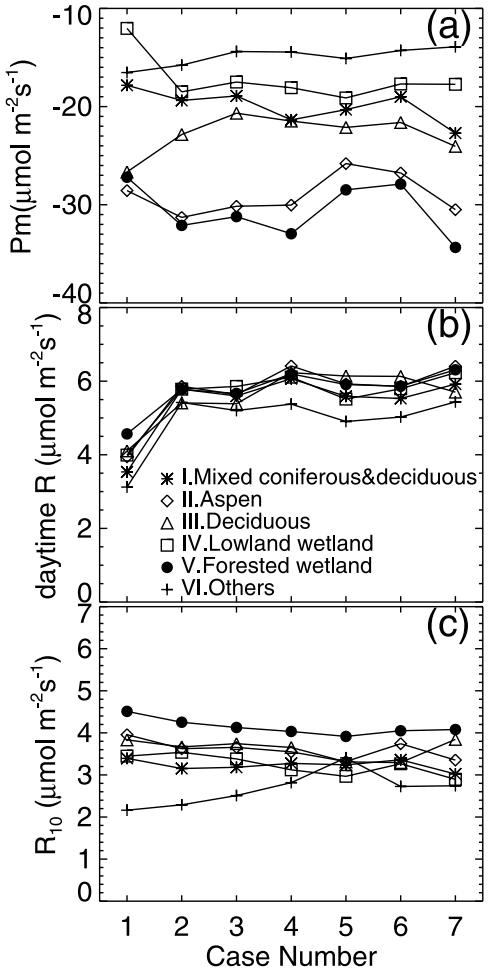

Figure 5. May through September averaged parameters of (a) P_m, (b) R_d in the light response model, and (c) R_{10} in the respiration model vary when the surface layer footprints are estimated using different z_0 and d values (see text). Case 1: $z_0 = 0.5$ m, $d = 15$ m; case 2: $z_0 = 0.4$ m, $d = 10$ m; case 3: $z_0 = 0.3$ m, $d = 8$ m; case 4: $z_0 = 0.2$ m, $d = 6$ m; case 5: $z_0 = 0.1$ m, $d = 4$ m; case 6: $z_0 = 0.2$ m, $d = 6$ m, σ_y is reduced by a factor of 2; case 7: $z_0 = 0.2$, $d = 6$ m, σ_y is doubled. Note that footprints for the measurements above the surface layer remain the same in all cases.

different horizontal diffusion coefficients in the instance of case 4, i.e., (6) $z_0 = 0.2$ m, $d = 6$ m, and σ_y is half of that in case 4; (7) $z_0 = 0.2$ m, $d = 6$ m, and σ_y is twice of that in case 4.

[44] Figure 5 compares the May through September averaged values of P_{max} and R_d in the light response model (equation (4)), and R_{10} in the respiration model (equation (5)) inferred using the surface layer footprints in the seven cases. The footprints for measurements above the surface layer remain the same. The differences in the seasonally-averaged P_{max} among ecosystem types are significant for all cases (Figure 5a). Overall, the results are fairly consistent across the ranges of z_0, d, and σ_y except for case 1. Assuming that the light-saturated assimilation and respiration rates for ecosystem VI (Table 1) would be the smallest among all ecosystems, the results of case 4 could be interpretable, which is reported in this manuscript as a case study. It should be pointed out that more advanced models should be used to simulate the footprint more precisely under this complex condition (inhomogeneous surface); this is one of priorities in the future efforts in order to apply the decomposition method described here in practice.

5. Discussion

5.1. Can WLEF Measurements Approximate Regional Fluxes? A Footprint Perspective

[45] From the perspective of footprints, we examine if flux measurements at the WLEF tower can be used to approximate the aggregated fluxes in the region. Eddy-covariance fluxes can be interpreted as the weighted averages of the fluxes from various stand types in the footprint areas (equation (2)). As an example, Figure 6 presents the mean weights (equation (3)) for daytime EC measurements at the three levels of the WLEF tower in the growing season in 2000. Note that footprints for measurements at 30 m under all unstable conditions are included in this calculation.

[46] The 30-m level is influenced significantly by the grassy clearing at the base of the tower. In contrast, the 122-m and 396-m footprint areas are mostly covered by the forested upland and wetland ecosystems. Owing to varying footprints (Figure 6), daytime flux with the 30-m footprint is roughly 2.4 μmol m^{-2} s^{-1} less negative than that with the 122-m footprint during the growing season, while daytime flux with the 122-m footprint is roughly 0.6 μmol m^{-2} s^{-1} less negative than that with the 396-m footprint. In this evaluation, we assume that all fluxes are measured in the surface layer (30 m) and PAR is 2000 μmol m^{-2} s^{-1}. The weights of the stand types sampled at 122 and 396 m are closer to the fractional areas of the stand types distributed in the region (Table 1) than at 30 m, implying

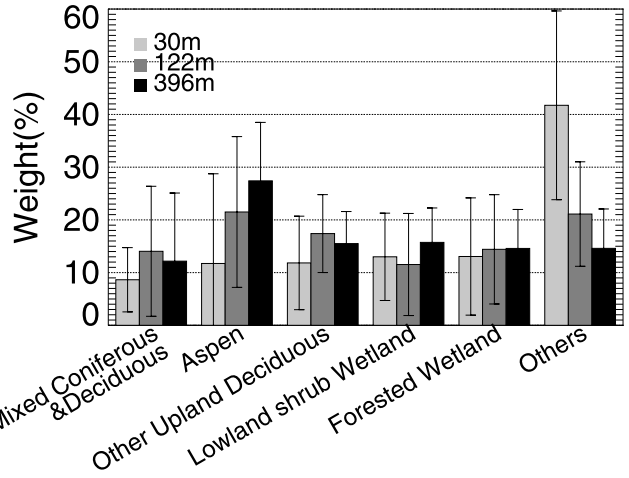

Figure 6. The mean weights of each stand type for daytime flux measurements from the three levels of the WLEF tower during May through September of the year 2000. The 30 m footprints are calculated under near-neutral to unstable conditions. When the acceptor heights are above the surface layer, as is often the case for 122 m and 396 m flux measurements, footprints are computed only for strongly unstable conditions. Each error bar represents the standard deviation of the calculated hourly weights during the season.

that daytime measurements at higher levels might be closer to the area-averaged fluxes in the region. Note that this analysis assumes that the six stand types we have chosen properly represent CO_2 fluxes in the region and that the horizontal advection impacts can be reduced after long-term average. The implication is consistent with that in a subsequent study that compares daytime NEE measurements at three levels of the WLEF tower with NEE inferred from a regional CO_2 budget method (W. Wang et al., submitted manuscript, 2005). In addition, footprints vary with time (1 order difference between daytime and nighttime) and hence the weights of stands to measured fluxes can change with time over this heterogeneous area. As a result, it is hard to interpret the temporally integrated (e.g., daily and yearly) NEE measurements at WLEF particularly when differences in NEE among stand types are significant. *Davis et al.* [2003] discussed this issue and proposed an algorithm for computing NEE with combination of three-level data.

5.2. Comparison of the Ecosystem Responses to Environmental Conditions at the Three Sites

[47] To extend tower measurements to the region, it is critical to assess whether NEE for each stand type in the WLEF footprint area and NEE measured at the WC and LC towers would be representative in the entire region or not. Choosing a classification scheme is one of the most important steps to make such an assessment. Two classification schemes are used in the following and possible implications are discussed.

5.2.1. Wetland-Upland Classification

[48] The upscaling hypothesis that the fluxes measured at the WLEF site are area-weighted averages of the fluxes measured at the LC and WC sites is utilized to assess whether the measurements at the two short towers can represent the NEEs for all the wetlands and uplands in the region, respectively. In this hypothesis, all ecosystems are categorized into upland or wetland ecosystems based on watershed functions (Table 1).

[49] According to this hypothesis, the average daily integrated GEP and ER at the WLEF site should be an intermediate value between those measured at the LC and WC sites, respectively. The hypothesis cannot be rejected for the average daily integrated GEP because the GEP at the WLEF is in between those at the two other sites. The data, however, show that the average daily ER measured at the WLEF site is larger than either of the other two sites (Figure 4). Consequently, there is no way the weighted mean of the observed ER at the WC and LC towers can equal that at the WLEF tower. The hypothesis must be rejected unless the error in the measurements is greater than the difference (unlikely in this case). The rejection of this hypothesis indicates that the watershed-function level of classification is insufficient for upscaling in the region. In other words, the responses of some stand types within the category of wetland, or within the category of forest upland, or both, to the same environmental conditions can be significantly different from one another, particularly in terms of respiration rates. Another implication from the rejection is that the fluxes could be different for the same stand types at different sites. Both implications are supported partially by the comparisons of the fluxes and functional parameters among stand types and among sites in section 4.2.

5.2.2. Six Stand Type Classification

[50] Since the watershed-function-based classification scheme is obviously insufficient, we hypothesize that regional fluxes can be described as an aggregate of fluxes for six different stand types, which is motivated in part by *Mackay et al.* [2002]. We evaluate this hypothesis by comparing the fluxes of some stand types in the WLEF footprint area to the WC and LC flux measurements.

[51] The ER values for stand types around the WLEF tower are larger than the stands of the same type sampled by the WC and LC towers. GEP values for the upland deciduous forests in the WLEF footprint area are smaller than that at the WC site. Therefore the magnitude of NEE at the WC site is larger than those of the upland deciduous forests around WLEF by a factor of about 3. These comparisons suggest that the ER and GEP measured at the WC site (an upland deciduous forest stand) are not representative of those of the upland deciduous forests in the WLEF footprint area. Unlike ER, GEP measured at the LC site is similar to that for the lowland wetlands in the WLEF footprint area. As a result, NEE at the LC site is more negative and cannot represent the lowland wetland ecosystem in the WLEF footprint area. These results suggest that a more detailed classification scheme is needed for both wetland and upland deciduous forest stand types. Another possible explanation is owing to errors in the flux decomposition, but the ER values are so different that it seems unlikely that such errors would resolve the discrepancies. Therefore the upscaling scheme based on the six stand type classification is still improper.

[52] The high ER measured at the WLEF tower might be in part due to the effects of the surrounding forested wetland and aspen ecosystems whose respiration rates are higher than others. The understory is sparse at the WC site compared to the WLEF site, likely accounting in part for the significant differences in the ER for the ecosystems with the upland deciduous forests at the two sites. Other reasons we do not rule out include the effects of other factors such as canopy age and density, tree roots, soil, and litter quality on the ecosystem respiration. Differences in GEP might be due to plant species, canopy density, micrometeorological conditions, and other biological factors. More observations are needed to specially identify the differences in stands that are critical to flux aggregation. Determining how to properly classify the ecosystem and design measurements is a challenge for the bottom-up method.

5.3. Aggregation Experiments

[53] Despite our inability to present a landscape classification scheme that reconciles WLEF flux data with those from WC and LC, it is instructive to construct a variety of aggregated flux measurements using these data. These aggregations present a quantitative measure of the uncertainty in regional fluxes that arises from the insufficient classification schemes. Spatially aggregated estimates of ER, GEP, and NEE are developed from the regional vegetation map and four different combinations of tower measurements and fluxes for the ecosystem types. In the first aggregation method, the watershed-function level classification is used. The ecosystems of the regional vegetation map are classified into two types, wetland or upland. Wetland fluxes are represented by LC site measurements

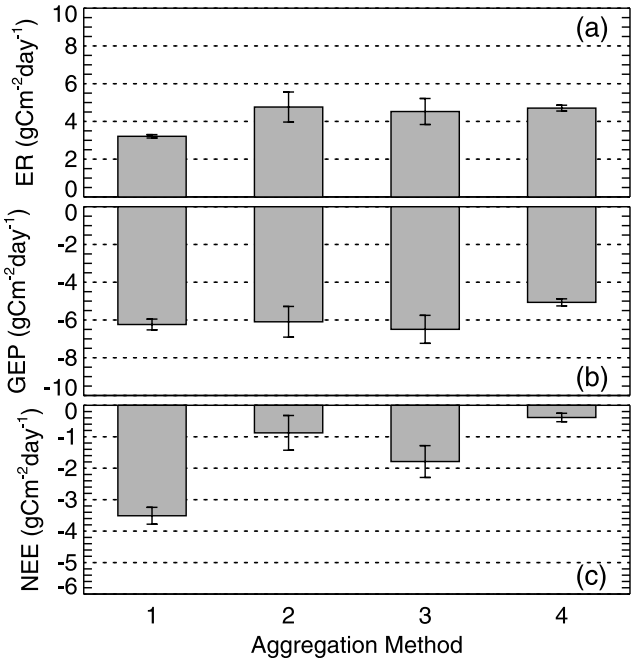

Figure 7. Daily integrated, aggregated fluxes averaged over the growing seasons (May through September) in 2003. (a) ER, (b) GEP, and (c) NEE from four aggregation methods (see section 5.3). The error bars are the standard deviations of the means; the uncertainty due to the classification data is not considered.

and upland fluxes are represented by WC site measurements. In the second aggregation method, the stand type level classification is used, where the inferred fluxes for the six ecosystem types (Table 1) in the WLEF footprint area are used to represent the entire region. The third aggregation method is the same as the second one, with the exception that WC data are used in place of the inferred flux for the upland deciduous forest ecosystem type flux (type III) and LC data are used in place of the inferred flux for lowland shrub wetlands (type IV). In the fourth method, the fluxes measured at the WLEF tower (see *Davis et al.* [2003] on how to compute WLEF NEE) are integrated directly and assumed to be regional estimates.

[54] Figure 7 compares the averaged daily integrated ER, NEE, and GEP for each method during the growing season in 2003. The aggregated daily ER is the lowest in method 1, while no significant difference is found among the other three methods. The magnitude of GEP estimated directly by integrating the WLEF tower data with time (method 4) is the smallest. There is no significant difference in GEP among the three aggregations. The large ER and small GEP result in the least negative NEE (smallest net uptake) from direct integration of the WLEF tower flux data (method 4). The large GEP and small ER result in the most negative NEE (largest net uptake) in method 1. We hypothesize that the results from method 3 might be the best estimates as the broadest sample of observations are included and the aggregated NEE is closest to that inferred from an independent top-down method [*Wang*, 2005, Figure 6.1]. Unless other stand types covering large areas and having fluxes falling out of the range of those presented here exist, aggregations 1 and 4 suggest bounds for the regional fluxes; the difference in the cumulative regional NEE estimate between these two aggregations is large, about 400 gC m^{-2} over the growing season. This large difference found among the small number of flux observations suggests that the range of fluxes among stands in this region is greatly undersampled in this study. This also shows the danger of using any single flux tower to describe a large region.

5.4. Limitations

[55] Application of the decomposition method developed here has several limitations. First, the accuracy of the classification inherent in the vegetation map is potentially important and has not been taken into account in this analysis. The overall accuracy is in the range of about 40% to 90% depending on classes [*WiDNR*, 1998]. Misclassification of stand type will cause errors in the flux decomposition and interpretation. The land cover data cannot reflect recent changes in vegetation caused by ongoing forest management and manipulation of water table depth. A more accurate inventory of the stand types would improve the representativeness of any aggregation and the interpretation of the measurements at the WLEF tower.

[56] Second, satellite remote sensors have difficulty detecting forest understory, litter, vegetation density, stand age, and stand height, all of which may be needed to describe the carbon exchange between forests and the atmosphere. It appears that ecosystem fluxes are dependent not only on stand type but also on those additional stand features, as suggested by this study and as shown by another study using additional stand-level flux measurements [*Desai et al.*, 2006]. Consequently, to aggregate the measured fluxes at towers more effectively, we need to consider classification schemes which go beyond land cover (focusing only on plant functional types) and take into account additional ecosystem variables. This study does not have enough data to define which variables must be included. Identifying the variables needed and mapping them accurately are challenges to the aggregation of carbon flux measurements.

[57] Third, the precision and accuracy of the derived functional parameters and fluxes are limited by the uncertainty of the simulated footprints, the ecosystem models, and flux measurements. The underlying flux decomposition is sensitive to the uncertainty of the eddy flux measurements, an uncertainty that is also difficult to evaluate accurately despite many discussions in the literature. Errors in the derived parameters can be resulted from the use of the equal weights for all measured fluxes in the calculation. The footprint models apply only over dynamically homogeneous surfaces; this is usually not met in practice. The footprint uncertainty introduced by applying the models over inhomogeneous surfaces cannot be quantified. In addition, the effects of change in wind direction with height on footprint estimates are not taken into account.

[58] Finally, using the decomposition method shown here is impractical if the number of the stand types that must be distinguished is too large. Larger stand type number results in more unknowns; the requirements of accuracy for the footprints, vegetation map, and flux measurements become higher and are more difficult to meet. Experiments suggest that results cannot be interpreted if the number is greater

than 6. In practice, this method is likely to be used in combination with other measurements or modeling.

6. Conclusions and Future Work

[59] An approach has been introduced to decompose tower-based EC fluxes into NEE for stand types in the flux footprint area. CO_2 fluxes for six stand types are inferred in a case study from the temporal flux series measured at the WLEF tower in northern Wisconsin. The fluxes and functional parameters of the six stand types in the WLEF footprint area are compared with each other and with those observed at the WC and LC sites. Regional fluxes with different aggregation schemes are compared. Implications from the case study, which may be worth mentioning, are summarized as follows.

[60] First, from the perspective of footprint, measurements at the WLEF tower may not be directly approximated as regional NEE since the weight of each stand type to the measured flux in the footprint area is different from the fractional coverage of the corresponding stand type in the region. It is hard to judge if temporally integrated measurements can approximate region fluxes due to time-dependent footprint over this heterogeneous area.

[61] Second, it is critical to distinguish wetlands from uplands for flux aggregation. Moreover, within the broad category of upland deciduous forests, aspen stands respond differently from other deciduous hardwoods to the same environmental conditions. There is also a distinction between lowland shrub wetlands and forested wetlands. With and without the stand type classification scheme and the difference between sites being considered, the difference in the (cumulative) aggregated NEE can be as large as 250 gC m^{-2} over the growing season.

[62] Third, the six stand classification scheme still does not capture all the variability in stand characteristics relevant to CO_2 exchange, though it is better than the wetland-upland scheme. Compared to the same stands around in the WLEF footprint area, higher magnitude of GEP and lower ER are found at the WC site, and slightly lower magnitude of GEP and lower ER are found at the LC site. These differences for the same stand types at different sites imply the flaw of the currently-used ecosystem classification scheme. Other factors such as canopy age and structure may be important in addition to land cover types.

[63] Finally, the growing season aggregate daily NEE values in 2003 are about -1.79 ± 0.51 gC m^{-2} using the stand-type classification scheme, -3.51 ± 0.27 gC m^{-2} using the watershed-function classification scheme (wetland and upland), and -0.38 ± 0.13 gC m^{-2} directly integrated from the WLEF data. These differences arise from the insufficient classification schemes.

[64] The ability to derive fluxes and ecosystem parameters that show reasonable distinctions among the stand types suggests that this decomposition method has succeeded in this application despite the numerous sources of uncertainty. This method has the potential for upscaling and interpreting flux measurements over heterogeneous areas. The precision and accuracy of the results are limited by the accuracy of the vegetation map, the estimated footprints, ecosystem models, and flux measurements. Future efforts to improve the proposed decomposition approach include: (1) quantifying uncertainties in the vegetation map, footprints, and flux measurements; (2) extending flux footprint research to measurements with heterogeneous flows and complex surface conditions and above the surface layer; (3) incorporating soil moisture into the ecosystem model for uplands and wetlands; and (4) developing suitable ecosystem classification schemes. More field measurements are needed to confirm the finding here. Also, implications in the study may help identify key ecosystem types and design field measurements in the region. Regarding regional NEE estimates, other independent approaches such as top-down approaches should be used with the bottom-up approach to provide more constraints.

[65] **Acknowledgments.** The authors wish to acknowledge the help of numerous field crew, technicians, engineers, and students involved in installation, maintenance, troubleshooting and data collection at all the sites, the University of Wisconsin Kemp Natural Resources Station for lodging and logistics support, Ronald Teclaw and the staff of the U.S. Department of Agriculture (USDA) U.S. Forest Service (USFS) North Central Research Station for site and data collection support, and land owners for allowing access to field locations, including the U.S. Forest Service (USFS), Chequamegon-Nicolet National Forest, and the Wisconsin Educational Communications Board, and Roger Strand, chief engineer for WLEF-TV. WLEF carbon dioxide mixing ratios, site infrastructure and maintenance are supported by Arlyn Andrews and the staff of the National Oceanic and Atmospheric Administration (NOAA) Earth System Research Laboratory (ESRL) Global Monitoring Division (GMD) Carbon Cycle Greenhouse Gases Group (CCGG). This research was funded in part by U.S. Department of Energy (DOE), Office of Science (BER), Terrestrial Carbon Processes program, grant number DE-FG02-03ER63681, DOE BER Midwestern Regional Center of the National Institute for Global Environmental Change (NIGEC) under cooperative agreement DE-FC03-90ER61010, DE-FG03-90ER61013, National Space and Aeronautics Administration, Science Mission Directorate, grant NNG05GD51G, and National Science Foundation Research Collaboration Network grant DEB-0130380. The authors thank the anonymous reviewers for their insightful suggestions and comments that helped us improve this manuscript.

References

Arya, S. P. (1999), *Air Pollution Meteorology and Dispersion*, 310 pp., Oxford Univ. Press, New York.

Bakwin, P. S., P. P. Tans, D. F. Hurst, and C. Zhao (1998), Measurements of carbon dioxide on very tall towers: Results of the NOAA/CMDL program, *Tellus, Ser. B*, *50*(5), 401–415.

Baldocchi, D., et al. (2001), FLUXNET: A new tool to study the temporal and spatial variability of ecosystem-scale carbon dioxide, water vapor, and energy flux densities, *Bull. Am. Meteorol. Soc.*, *82*(11), 2415–2434.

Berger, B. W., K. J. Davis, C. Yi, P. S. Bakwin, and C. L. Zhao (2001), Long-term carbon dioxide fluxes from a very tall tower in a northern forest: Flux measurement methodology, *J. Atmos. Oceanic Technol.*, *18*, 529–542.

Bousquet, P., P. Monfray, P. Ciais, P. Peylin, and M. Ramonet (1999), Inverse modeling of annual atmospheric CO_2 sources and sinks: 1. Method and control inversion, *J. Geophys. Res.*, *104*(21), 26,161–26,178.

Burrows, S. N., S. T. Gower, M. K. Clayton, D. S. Mackay, D. E. Ahl, J. M. Norman, and G. Diak (2002), Application of geostatistics to characterize leaf area index (LAI) from flux tower to landscape scales using a cyclic sampling design, *Ecosystems*, *5*(7), 667–679.

Cao, M., and F. I. Woodward (1998), Net primary and ecosystem production and carbon stocks of terrestrial ecosystems and their responses to climate change, *Global Change Biol.*, *4*(2), 185–198.

Chen, J. M., J. I. MacPherson, S. G. Leblanc, J. Cihlar, and R. L. Desjardins (1999), Extending aircraft- and tower-based CO_2 flux measurements to a boreal region using a Landsat thematic mapper land cover map, *J. Geophys. Res.*, *104*(14), 16,859–16,877.

Ciais, P., R. J. Francey, P. P. Tans, M. Trolier, and J. W. C. White (1995), A large Northern Hemisphere terrestrial CO_2 sink indicated by the $^{13}C/^{12}C$ ratio of atmospheric CO_2, *Tellus, Ser. B.*, *269*(5227), 1098–1102.

Cook, B. D., et al. (2004), Carbon exchange and venting anomalies in an upland deciduous forest in northern Wisconsin, USA, *Agric. For. Meteorol.*, *126*(3–4), 271–295.

Cramer, W., et al. (2001), Global response of terrestrial ecosystem structure and function to CO_2 and climate change: Results from six dynamic global vegetation models, *Global Change Biol.*, *7*(4), 357–373.

Davis, K. J., P. S. Bakwin, C. Yi, B. W. Berger, C. Zhao, R. M. Teclaw, and J. G. Isebrands (2003), The annual cycles of CO_2 and H_2O exchange over a northern mixed forest as observed from a very tall tower, *Global Change Biol.*, *9*(9), 1278–1293.

Desai, A. R., et al. (2006), Influence of vegetation type, stand age and climate on carbon dioxide fluxes across the upper Midwest, USA: Implications for regional scaling of carbon flux, *Agric. For. Meteorol.*, in press.

Enting, I. G. (2002), *Inverse Problems in Atmospheric Constituent Transport*, 392 pp., Cambridge Univ. Press, New York.

Enting, I. G., C. M. Trudinger, and R. J. Francey (1995), A synthesis inversion of the concentration and $\delta^{13}C$ of atmospheric CO_2, *Tellus, Ser. B*, *47*(1–2), 35–52.

Gurney, K. R., et al. (2002), Towards robust regional estimates of CO_2 sources and sinks using atmospheric transport models, *Nature*, *415*(6872), 626–630.

Horst, T. W. (1979), Lagrangian similarity modeling of vertical diffusion from a ground-level source, *J. Appl. Meteorol.*, *18*(6), 733–740.

Horst, T. W., and J. C. Weil (1992), Footprint estimation for scalar flux measurements in the atmospheric surface layer, *Boundary Layer Meteorol.*, *59*(3), 279–296.

Horst, T. W., and J. C. Weil (1994), How far is far enough? The fetch requirements for micrometeorological measurement of surface fluxes, *J. Atmos. Oceanic Technol.*, *11*, 1018–1025.

Horst, T. W., and J. C. Weil (1995), Corrigenda, *J. Atmos. Oceanic Technol*, *12*, 447–448.

Huntingford, C., P. M. Cox, and T. M. Lenton (2000), Contrasting responses of a simple terrestrial ecosystem model to global change, *Ecol. Modell.*, *134*(1), 41–58.

Intergovernmental Panel on Climate Change (2001), *Climate Change 2001: The Scientific Basis—Contribution of Working Group I to the Third Assessment Report of the Intergovernmental Panel on Climate Change*, 881 pp., Cambridge Univ. Press, New York.

Lloyd, J., and J. A. Taylor (1994), On the temperature dependence of soil respiration, *Funct. Ecol.*, *8*(3), 315–323.

Luo, Y., D. Hui, W. Cheng, J. S. Coleman, D. W. Johnson, and D. A. Sims (2000), Canopy quantum yield in a mesocosm study, *Agric. For. Meteorol.*, *100*(1), 35–48.

Mackay, D. S., S. N. Burrows, S. Samanta, K. J. Davis, D. E. Ahl, B. E. Ewers, and S. T. Gower (2002), Effects of aggregated classifications of forest composition on estimates of evapotranspiration in a northern Wisconsin forest, *Global Change Biol.*, *8*(12), 1253–1265.

Nilsen, E. T., and M. R. Sharifi (1994), Seasonal acclimation of stem photosynthesis in woody legume species from the Mojave and Sonoran deserts of California, *Plant Physiol.*, *105*(4), 1385–1391.

Ogunjemiyo, S. O., R. L. Desjardins, D. A. Roberts, S. K. Kaharabata, P. H. Schuepp, and I. J. MacPherson (2003), Methods of estimating CO_2, latent heat and sensible heat fluxes from estimates of land cover fractions in the flux footprint, *Agric. For. Meteorol.*, *117*(3–4), 125–144.

Ott, L. (1993), *An Introduction to Statistical Methods and Data Analysis*, 132 pp., Duxbury, Pacific Grove, Calif.

Pan, Y., et al. (1998), Modeled responses of terrestrial ecosystems to elevated atmospheric CO_2: A comparison of simulations by the biogeochemistry models of the Vegetation/Ecosystem Modeling and Analysis Project (VEMAP), *Oecologia*, *114*(3), 389–404.

Reichstein, M., J. D. Tenhunen, O. Roupsard, J.-M. Ourcival, S. Rambal, S. Dore, and R. Valentini (2002), Ecosystem respiration in two Mediterranean evergreen Holm Oak forests: Drought effects and decomposition dynamics, *Funct Ecol.*, *16*(1), 27–39.

Ricciuto, D. M., M. P. Butler, K. J. Davis, B. D. Cook, P. S. Bakwin, A. E. Andrews, and R. M. Teclaw (2006), A Bayesian synthesis inversion of simple respiration and GEO models with eddy covariance data in a northern Wisconsin forest: Determining the causes of interannual variability, *Agric. For. Meteorol.*, in press.

Rodgers, C. D. (2000), *Inverse Methods for Atmospheric Sounding: Theory and Practice*, 238 pp., World Sci., Hackensack, N. J.

Ruimy, A., P. G. Jarvis, D. D. Baldocchi, and B. Saugier (1995), CO_2 fluxes over plant canopies and solar radiation: A review, *Adv. Ecol. Res.*, *26*, 1–68.

Schmid, H. P. (2002), Footprint modeling for vegetation atmosphere exchange studies: A review and perspective, *Agric. For. Meteorol.*, *113*(1–4), 159–183.

Schuepp, P. H., M. Y. Leclerc, J. I. Macpherson, and R. L. Desjardins (1990), Footprint prediction of scalar fluxes from analytical solutions of the diffusion equation, *Boundary Layer Meteorol.*, *50*(1–4), 355–373.

Tans, P. P., I. Y. Fung, and T. Takahashi (1990), Observational constraints on the global atmospheric CO_2 budget, *Tellus, Ser. B*, *247*(4949), 1431–1438.

van Ulden, A. P. (1978), Simple estimates for vertical diffusion from sources near the ground, *Atmos. Environ.*, *12*, 2125–2129.

Wang, W. (2005), Regional estimates of net ecosystem-atmosphere exchange of carbon dioxide over a heterogeneous ecosystem, dissertation thesis, Penn. State Univ., University Park.

Wang, W., K. J. Davis, D. M. Ricciuto, and M. P. Butler (2004), Footprint modeling for flux measurements at multiple levels from a very tall tower over a mixed forest, paper presented at 16th Symposium on Boundary Layer and Turbulence, Am. Meteorol. Soc., Portland, Maine. (Available at http://ams.confex.com/ams/pdfpapers/78934.pdf)

Wang, W., K. J. Davis, B. D. Cook, P. S. Bakwin, C. Yi, M. P. Butler, and D. M. Riccinto (2005), Surface layer CO_2 budget and advective contributions to measurements of net ecosystem-atmosphere exchange of CO_2, *Agric. For. Meteorol.*, *135*(1–4), 202–214.

Wisconsin Department of Natural Resources (1998), WISCLAND land cover, *WLCGW930*, Madison, Wis.

Woodward, F. I., and C. K. Kelly (1995), The influence of CO_2 concentration on stomatal density, *New Phytol.*, *131*(3), 311–327.

Woodward, F. I., J. A. Lake, and W. P. Quick (2002), Stomatal development and CO_2: Ecological consequences, *New Phytol.*, *153*(3), 477–484.

Yi, C., K. J. Davis, B. W. Berger, and P. S. Bakwin (2001), Long-term observations of the dynamics of the continental planetary boundary layer, *J. Atmos. Sci.*, *58*(10), 1288–1299.

M. P. Butler, K. J. Davis, and D. M. Ricciuto, Department of Meteorology, Pennsylvania State University, 503 Walker Building, University Park, PA 16802-5013, USA.

B. D. Cook, Department of Forest Resources, University of Minnesota, 1530 North Cleveland Avenue, Saint Paul, MN 55108, USA.

W. Wang, Pacific Northwest National Laboratory, P.O. BOX 999, K9-30, Richland, WA 99352, USA. (wang@met.psu.edu)